Transaction A: Civil Engineering
Vol. 16, No. 1, pp. 78–86

SCIENTIA IRANICA

On the Distribution of Velocity in a V-Shaped Channel

M.A. Mohammadi[1]

Abstract. *Several series of measurements were conducted to explore the hydraulic characteristics of a V-shaped bottom channel by using low & high-speed velocity propellers for point-wise velocity measurements. Also, in order to understand the effect of cross sectional channel shape on the distribution of depth-averaged velocity in the experimental channel, cases with different flow rates were examined. Using SURFER software, the contour plots of 2D isovels were drawn as interpolation among averaged depths and velocities, obtained from superposing the various profile sections. It was observed that isovels are parallel to the channel boundary in a region close to the bed, and almost symmetric about the centerline, with some deviations. The variation of point velocities in each slice considered along a spanwise direction, in order to study the depthwise velocity profile distributions, is shown. The lateral variations of depth-averaged velocities indicate that the velocity distributions are almost symmetrical about the cross sectional centerline, except for some flow cases, in which there are slight deviations, despite the fact that the flow condition was uniform for all cases. It was found that the widely used log-law for the vertical profile of velocity does not appropriately model the velocity distribution in this particular channel shape. Considering the results obtained for the span- and depth-wise velocity distributions, especially the distortion of the isovels and the location of maximum velocity, there are strong evidences of secondary currents that are present in this channel cross section.*

Keywords: *V-shaped bottom channel; Uniform flow; Velocity distribution; Depth-averaged velocity; Boundary shear stress.*

INTRODUCTION

When a fluid passes over a solid boundary, the boundary exerts a force on the fluid, which is magnified by a reduction in the fluid viscosity. The reduction in velocity becomes less apparent as the distance from the surface increases. The varying flow velocity region next to the solid boundary is referred to as a boundary layer. For a smooth surface, the boundary layer can be divided into three regions, namely, laminar, transitional and turbulent. Figure 1 illustrates these regions by considering a hypothetical flat plate that is immersed in a flowing fluid (see [1,2] for more details).

The local and depth-averaged velocities are used to predict the velocity distribution and an exact estimate of the discharge and friction in open channels. The skin friction coefficient for the sloping smooth surface tests were measured by Balachandar et al. [3]. They found that this coefficient tends to be slightly higher than that observed for the flow over a horizontal surface. As indicated by the wake function, Ω, the free surface, the channel slope and the roughness of the channel affect the outer region of the boundary layer [4]. According to Knight et al. [5] the method of Shiono & Knight [6] offers a new approach in calculating the lateral distributions of the depth-averaged velocity and boundary shear stress for flows in straight prismatic channels. It accounts for bed shear, lateral shear and secondary flow effects; thus, incorporating some key 3D flow features into a lateral distribution model for streamwise motion. However, recent research work in open channels (see e.g. [3,5,7-22]) all emphasize that the velocity still needs to be explored for open channel cross sections separately. This paper presents new experimental data collected for a V-shaped bottom channel cross section, together with the analysis of the results and conclusions obtained.

1. *Department of Civil Engineering, Urmia University, P.O. Box 57169-33111, Urmia, Iran. E-mail: m.mohammadi@mail.urmia.ac.ir*

Received 25 January 2007; received in revised form 8 August 2007; accepted 28 April 2008

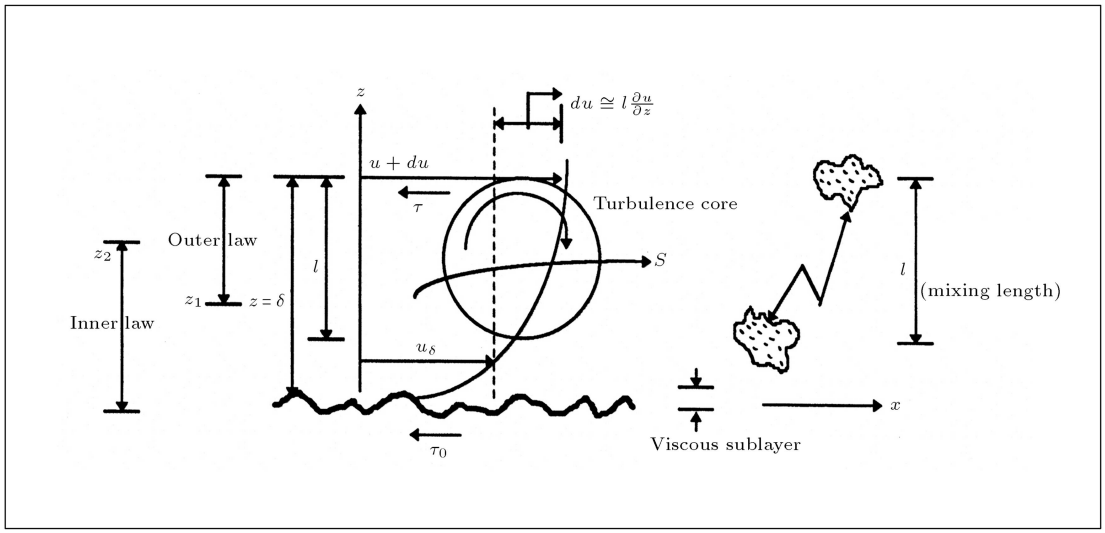

Figure 1. Regions of boundary layer inner and outer laws, and logarithmic velocity profile for a rough boundary, together with the turbulent mixing-length [1,2].

EXPERIMENTAL APPARATUS AND PROCEDURE

To investigate the hydraulic characteristics of a V-shaped bottom channel (see Figure 2), point velocity and boundary shear stress were measured in several series of the experiments. The described experimental channel was built inside the existing 15 m long tilting flume. Low and high speed velocity propellers were used for measuring point velocities and a Preston tube was used for measuring dynamic pressures to evaluate the boundary shear stress. Uniform flow was established using stage-discharge curves and discharge-tailgate relationships. The flume was supported by two hydraulic jacks and rotated about a hinge joint beneath the middle of the channel. The flume also had a motorized slope control system with a mechanical visual read out on a ruler at the upstream end of the flume, used for determining the precise channel bed slope. The maximum slope obtainable was $S_0 = 2\%$. The experimental channels, with a V-shaped bottom cross section built by using PVC panels to make a

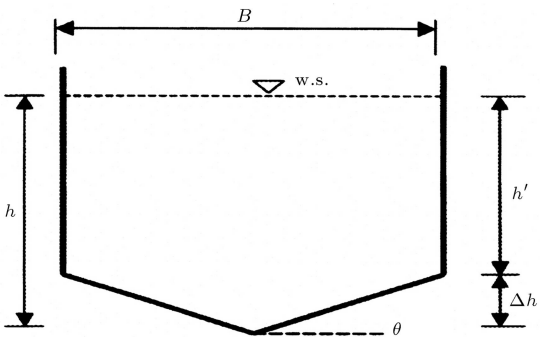

Figure 2. V-shaped bottom channel cross-section.

14.5 m long channel having a 50 mm crossfall, were built along the inside centerline of the existing flume.

Water was supplied to the channel by an overhead tank through a 101.6mm pipeline for flows up to 30 l/s and a 355.6 mm pipeline for discharges higher than 30 l/s. To reduce large-scale disturbance, and in order to ensure that the flow was uniformly distributed, a system of honeycombing was placed at the upstream end of the channel where the entrance tank and bell-mouth shaped inlet transition section were located. However, for the case of supercritical flow, i.e. Fr> 1, the honeycomb was not very useful, because of developing the S2 water surface profile. Individual bell-mouth shaped transition sections were designed and made for each channel type and served to reduce separation and improve the development of the mean flow into the channels. Flow measurements (up to 30 l/s) were made by means of a Venturi meter connected to mercury and air/water manometers at the upstream end of the flume. An electromagnetic flow meter was also installed in the supply line after the Venturi and was used to measure flows at the upstream. For the case of higher flows, a Dall-tube connected to an air/water manometer was used in the 355.6 mm diameter supply line. The flume has a very rigid bottom designed specifically to tolerate large loads and, therefore, it was not necessary to do deflection tests. A slatted tailgate weir was installed in the downstream of the channel, in order to minimize upstream disturbance of the flow and, hence, allowed a greater reach of the channel to be employed for experimental measurement in subcritical flows. The test section was 12 m long, commencing at a distance of 1.25 m from the channel entrance and 1.85 m from the flume entrance. However, for supercritical flows,

because of the S2 profiles, the test length was reduced to about 7 m. A trolley was mounted on rails running along the flume with a depth probe, having an electrical contact to the water surface level (accurate to 0.1 mm) and, hence, the channel bed slope was obtained. It has also been possible to do lateral measurements using the same trolley. The depth was measured at one and sometimes, half a meter intervals in the test length by means of a centerline pointer probe moved down from the instrument carriage.

Local velocity measurements were carried out by using the propeller technique with two Nixon 14 mm low and high speed propellers, namely, type 403 serial No 1976 low speed, and type 404 serial No 1981 high speed. The related calibration equations are:

$$u = 0.0063N - 0.0112, \tag{1}$$

for low speed probe type 403, and:

$$u = 0.0194N - 0.0394, \tag{2}$$

for high speed probe type 404.

The probe was mounted on a carriage and aligned vertically inside the water flow and normal to the bed. It was placed on the channel every 10 mm intervals on the vertical lines and every 20 mm intervals in a spanwise direction. The velocity numbers (N) were recorded by connecting the propeller to a simple indicator. The reading numbers were applied to assess the primary velocities using Equations 1 and 2.

For every set of flows, both point velocities in cross section and dynamic pressures in contact with the channel boundary were measured for the same flow condition. For both velocity and boundary shear stress, the data are analyzed from a variety of different perspectives, and the results from each analysis are used to interpret the mechanics occurring in the flow [23]. The findings from each perspective complement each other and highlight the consistency of the experimental data.

VELOCITY MEASUREMENTS RESULTS, ANALYSIS AND DISCUSSION

Primary Velocities

In order to explore the distribution of depth-averaged velocity in a V-shaped bottom channel, some measurements of point velocities were taken for different flow rates. A propeller indicator was set on 10 seconds and at least five numbers were recorded. Those five numbers were then averaged and obtained for evaluating the primary point velocities. Applying a corresponding calibration equation for any propeller, the point velocities were obtained. Point velocities were measured at a number of vertical sections normal to the bed along the transverse direction, in order to cover as much of the cross section as possible at 20 mm or 10 mm intervals. For flow discharges up to 30 ls^{-1}, an electro-magnet flow meter was used and, for flows higher than 30 ls^{-1}, a Dall tube was used for flow measurement. The local point velocities were multiplied by the surrounding subareas and the resulting curves were integrated over each vertical slice, from which the integrated discharge, $Q_{\mathrm{int.}}$, was obtained. The electro magnet flow meter discharge, $Q_{\mathrm{em.}}$, and Dall tube discharge, $Q_{\mathrm{dall.}}$, were then compared with the integrated discharges obtained from velocity measurements. The percentage error values of discharges were calculated as:

$$\%Q_{\mathrm{err}} = \frac{Q_{\mathrm{int}} - Q_{\mathrm{em/dall}}}{Q_{\mathrm{em/dall}}} \times 100. \tag{3}$$

Depth-averaged velocities were then adjusted to the em/dall mean values, so that when integrated they gave $Q_{\mathrm{int.}} = Q_{\mathrm{em/dall}}$. For large flow depths, the calculated error was in a very acceptable range, typically less than 2%. However for larger depths, the error was larger and reached up to 4% for a depth of 247.5 mm. Overall, the percentage error values are reasonably satisfactory.

2D Isovel Plots

In order to transform the point velocities to 2D isovel diagrams, a commercial software package, known as SURFER-2003, Golden Software, Inc., was used. The contour plots were drawn by interpolating averaged depths and velocities at a given position, obtained from superposing the various profile sections. The errors due to the averaging velocities and depths at a given point or section were not significantly different from any extreme values of depth and velocity at a measured point or section. However, one of the drawbacks with this software is that the calculations and diagrams are done assuming a computational square mesh, i.e. a rectangular channel cross section. This can provoke problems when the geometry of the channel is not easily represented by this approach. Although, this does not affect the overall accuracy of the interpolation, the use of a rectangular mesh produces a non smooth boundary when the results are viewed graphically. It also implies that the isovels near the channel boundary only approximately represent the actual distributions. However, from a quantitative point of view, the software is adequate. To solve this problem, a series of data were produced representing the channel boundary at small intervals along the wetted perimeter, and they were replaced as a channel boundary having zero velocities. The channel boundary is, therefore, viewed reasonably well. One of the representative 2D isovel plots for a flow discharge, $Q = 125.89\ \mathrm{ls}^{-1}$, at a channel bed slope, $S_0 = 0.2\%$, is shown plotted in Figure 3.

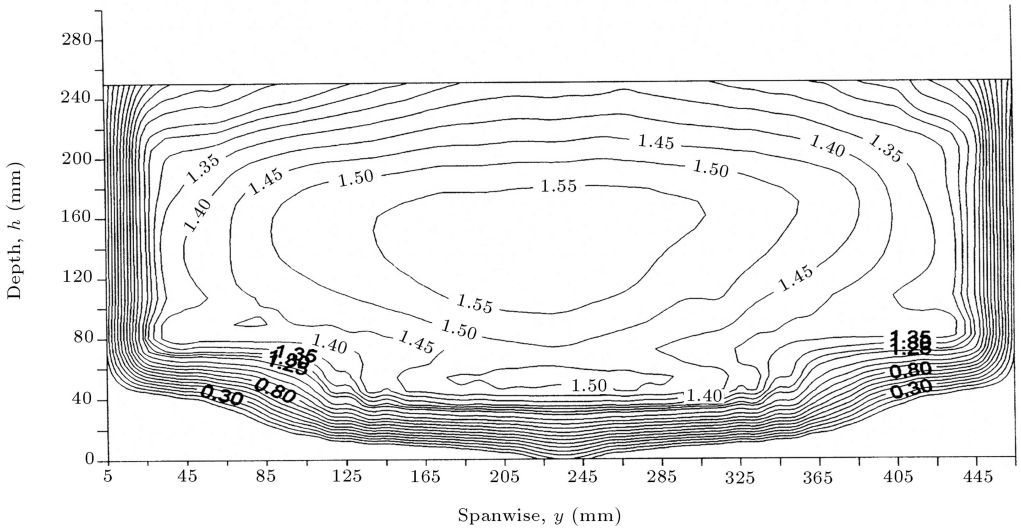

Figure 3. An example of isovel plot for a V-shaped channel: $Q = 125.89\ \mathrm{ls}^{-1}$ and $S_0 = 0.2\%$.

The primary point velocities were normalized by the section mean velocity, U, and plotted in a similar manner. A complete set of the results is presented by Mohammadi [2]. All the isovel plots illustrate the presence of steep velocity gradients close to the channel boundary, a feature that is the characteristic of turbulent boundary layer flow. It is seen that the isovels are parallel to the channel boundary in a region close to the bed and almost symmetric about the centerline. The plotted isovels (e.g. Figure 3) indicate that, as the flow depth increases and the channel gets steeper, the isovel patterns become more distorted and the position at which maximum isovel value occurs is depressed below the water surface. From the sediment transport point of view, this phenomenon causes more lift and erosion on the bed particles and, hence, more sediment movement [24].

The distortion of the isovels and the location of maximum velocity are strong evidence of secondary currents being present in this V-shaped bottom channel. The discontinuity between the V-shaped bottom part of the channel and the vertical walls is responsible for those distortions producing anisotropic turbulence. In cases of steeper channel beds, Fr> 1, the isovel plots are compressed towards the corner regions [2]. This result suggests that the momentum is being transported towards the corners. This phenomenon can be seen in the data and isovel contours given by Powell & Posey [25,26], for triangular 90°channels and, also, in [27] for the vertical walled shallow triangular channels. No explanation was offered by them. It has also been noted by Tominaga et al. [28] for trapezoidal channels. Tominaga et al. [28], however, proposed that this may be related to the bed generated vortex and the free surface flow. A strong water surface phenomenon resulted by the flow structure is also observable throughout the isovels plots. It can be seen that the distortions in the isovels increase as the flow depth increases and the channel gets steeper. This is likely to be linked to the number of secondary flow cells. If the secondary flow patterns could be drawn accurately from direct measurements of V and W, precise conditions could be drawn.

VERTICAL DISTRIBUTION OF LOCAL VELOCITIES AND PREDICTION OF FRICTION VELOCITIES

The variation of point velocities in each slice considered along the transverse direction in order to study the vertical velocity distributions is shown in Figure 4. The profiles are plotted from the wall towards the channel centerline. As can be seen from this figure, when profiles are going close to the flow surface, they tend towards the centerline part of the channel cross section. This again indicates the strong presence of secondary currents.

It is customary to compare velocity profiles with the universal logarithmic velocity law. In order to do this, the local velocity, u_i, must be normalized by the subsection friction velocity, u_{*i}, i.e. by u_{*w}, for the velocities normal to the walls and by u_{*b} for velocities normal to the bed: in order to give value of u^+, where $u^+ = u/u_{*i}$. The depth levels, z, at which velocities were measured, must also be normalized, as $u_{*i}z/\nu$ for velocities over smooth surfaces and as $z^+ = z/k_s$ for velocities over rough boundaries. The local boundary shear velocity, u_{*l}, can be calculated by using a semi-logarithmic relationship between the local velocities and related depths. For this purpose, the following equation may be applied:

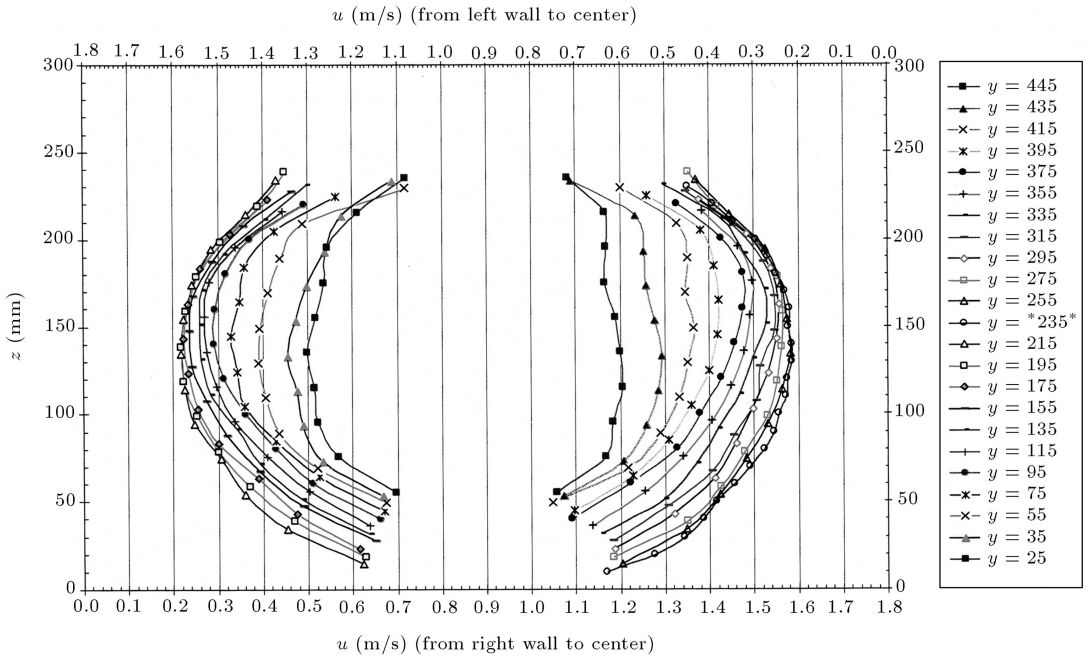

Figure 4. Velocity profiles over the depth, z, at different spanwise positions, y, in a V-shaped channel: $Q = 125.89$ ls^{-1} and $S_0 = 0.2\%$.

$$u_{*l} = \frac{M_s \kappa}{2.303}, \tag{4}$$

where M_s is the regression coefficient and κ is the Karman constant, taken in this study as $\kappa = 0.41$, suggested by Nezu & Rodi [29]. Then, the local shear stress is estimated by:

$$\tau_l = \rho u_{*l}^2. \tag{5}$$

However, it was not possible to apply this approach, because the above mentioned relationship in Equation 4 did not give a reasonable value for M_s with which to evaluate the local friction velocities. Instead, the boundary shear stress results were used to estimate the local friction velocities, where the flow conditions for boundary shear stress were the same as for the velocity measurements. For the V-shaped bottom channel, this process was carried out and the results were used for log-law examination.

Using the local boundary shear stress measurements, the adjusted values of shear velocity, $u_{*l} = \sqrt{\tau_l/\rho}$, were tabulated and used to compare the experimental relating data with the universal velocity law. The variation of normalized point velocities, $u^+ = u/u_{*l}$ at $y = 75$, 155, 235, 315 and 395 mm along a spanwise direction, are shown plotted versus $\ln(z^+)$ in Figure 5. The universal logarithmic velocity law coefficients used by Nezu & Rodi [29] are $A = 2.427$ & $B = 5.29$.

It is clear that the experimental results are not consistent with the universal logarithmic velocity law,

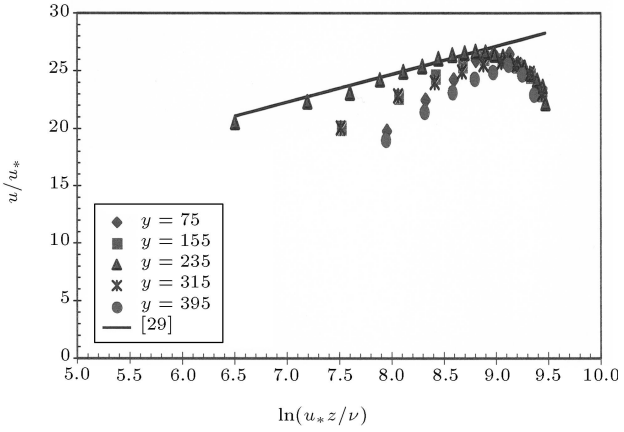

Figure 5. u/u_* versus $\ln(u_* z/\nu)$ at different spanwise positions, y : $Q = 125.89$ l/s & $S_0 = 0.2\%$.

as might be expected. As can be seen from the figures, likewise Figure 5, the universal log-law only matches some parts of the velocity profiles under some flow conditions. For example, it lies on the centerline profile at $Q = 25.03$ ls^{-1} & $S_0 = 0.9\%$ and, for the case of $Q = 50.931$ ls^{-1} & $S_0 = 0.4\%$, it matches a little with profiles in $y = 155$ & 355 mm positions. However, in some cases of flow, the universal law is far from in agreement with the experimental data (see [2]). As expected, the strong effects of cross sectional shape and secondary currents on the flow behavior in this particular channel shape cause the relating distributions to deviate from their simple 2D distribution law.

LATERAL DISTRIBUTION OF DEPTH-AVERAGED VELOCITIES, U_D

Integrating the local velocities, u, over the flow depth, h, gives the depth-averaged velocity, U_d. As an example, Figure 6a shows the lateral variations of depth-averaged velocities and also their normalized distributions for different flow discharge and slope settings. The section mean velocities are also shown as solid lines related to every flow test on the same figures. It can be seen from these figures that the distributions are almost symmetrical about the cross sectional centerline, but they deviate for some flow cases, despite the flow condition being uniform for all cases. At large flow depths, the maximum velocity occurs at the centerline and reduces continuously towards the sidewalls, indicating that the sidewalls exert a large influence on flow behavior. These data would be useful for validating various computational models, such as the 2D depth-averaged model given by Shiono & Knight [6]. The measured depth-mean velocities were also normalized by section mean velocity, U_d/U, and plotted versus spanwise direction, y, for some selected flow tests, as shown in the figures, likewise Figure 6b. It can be seen from this figure that some deviations are observable. This leads to the view that the secondary current cells affect the flow behavior.

LOCATION OF MAXIMUM VELOCITY AND ITS RELATION WITH SECTION MEAN VELOCITY, U

In open channel flows, the maximum velocity, $u_{\max}$, and its location in a channel cross section, as well as the mean velocity, $U(= Q/A)$, is a valuable parameter. However, it is mentioned very little. The location of the maximum velocity in a channel cross section depends upon the shape of the channel cross section and, consequently, it depends upon the resultant effects

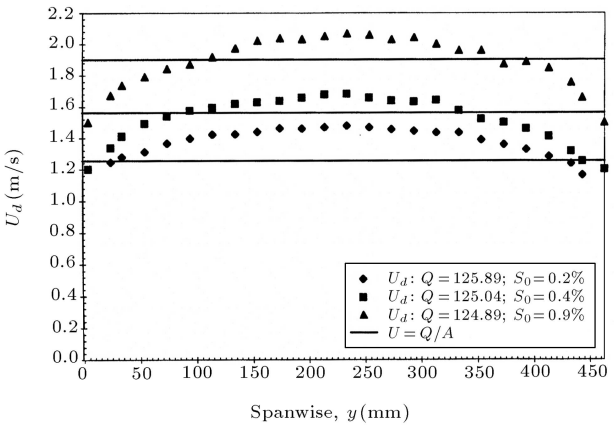

Figure 6a. Lateral distribution of depth-averaged velocity in a V-shaped channel: $Q = 125$ ls^{-1}.

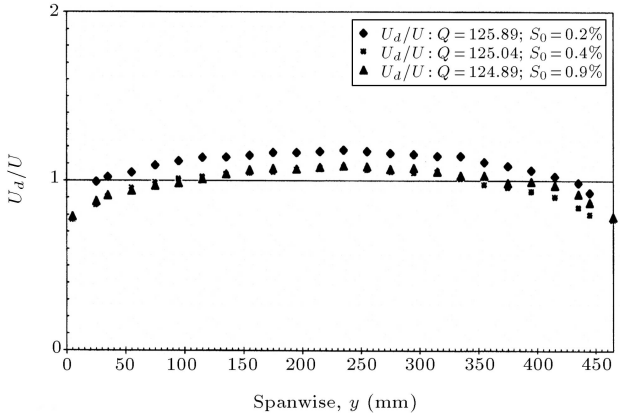

Figure 6b. Dimensionless lateral distribution of depth-averaged velocity in a V-shaped channel: $Q = 125$ ls^{-1}.

of the secondary currents. The relation between U and $u_{\max}$ for pipe flows in most textbooks is referred to as:

$$\frac{U}{u_{\max}} = c, \tag{6}$$

where c is a constant and is equal to 0.8167 (see [30]). This relationship can be achieved by using the Prandtl (1/7th) velocity distribution law in a circular pipe as follows:

$$\frac{u}{u_{\max}} = (z/r_0)^{1/7}, \tag{7}$$

in which u is the point velocity at a depthwise distance, z, from the pipe wall and r_0 is the pipe radius.

As is well known, the velocity entropy profile derived by Chiu [31] is based on the probabilistic approach and represents a very useful tool for researchers and engineers, because it is founded on few synthetic parameters relatively easy to derive. Chiu [32-36] have studied the velocity distribution in either pipe flows or open channel flows and, by applying the entropy concept, they have given the following equation to describe the ratio, c:

$$\frac{U}{u_{\max}} = \frac{e^M}{e^M - 1} \cong \frac{1}{M} = c, \tag{8}$$

where M is the dimensionless entropy parameter ($M = 1/c = 1.2244$ for pipe flows and does not satisfy the approximate equality very well). According to Chiu & Said [36,37] the measurable maximum velocity can be considered as a 'single' value, from which one can know the range of the velocity in a channel cross section and, furthermore, obtain useful information about the type of open channel flow. The above relationship between U and $u_{\max}$ was examined by Xia [38] for a natural river, i.e. the Mississippi River and by Sterling [39] for a part-full pipe channel. They found that there is a linear relationship between $u_{\max}$ and U. It may

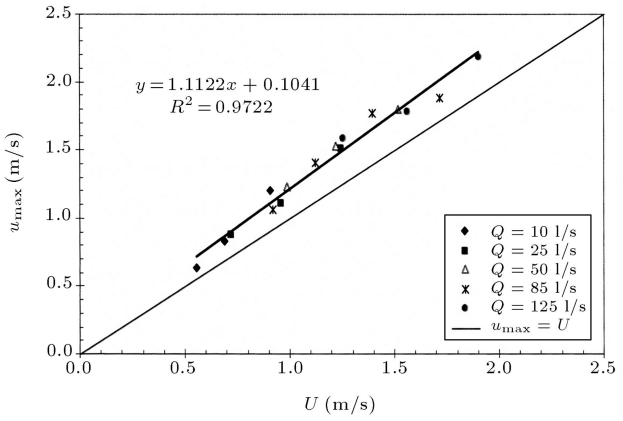

Figure 7. Variation of maximum velocity values in a V-shaped channel for different flow discharges.

be concluded that, for natural rivers and man-made channels, the maximum velocity might play a useful role, but not as important a role as U. For open channel flows of different cross sectional shapes, not only does the constant number, c or M, vary, but also the location of the maximum velocity does alter. This makes the use of u_{max} somewhat problematic.

In order to determine the location of the maximum velocity and its relationship with section mean velocity, U, for different flow conditions, Figure 7 was constructed. Figure 7 illustrates that there is a good linear relationship between u_{max} and U, given by:

$$u_{max} = 1.1122U + 0.1041, \qquad (R^2 = 97.22\%). \qquad (9)$$

Employing a least square analysis on the data and imposing the condition that the trend line is set to zero, i.e. when $U = 0$, then, $u_{max} = 0$ and the following is obtaine:

$$u_{max} = 1.1934U, \qquad (R^2 = 97\%). \qquad (10)$$

A comparison of Equations 8 and 10 gives constant parameter values as: $c = 0.8379$ and $M = 1.1934$. This result confirms that, for a V-shaped bottom channel, the value of dimensionless entropy parameter, M, is lower than that of the standard value for circular pipe flows. The position of maximum velocity in the spanwise direction was produced. It was seen from Figure 7 that the majority of the data lies on the central slice of the cross section at $y = 230$ mm, with only a few data positioned in two neighboring slices.

CONCLUDING REMARKS

The point velocity measurements have been undertaken in the uniform flow condition for five target flow discharges of 10, 25, 50, 85 & 125 ls^{-1} , at four different channel bed slopes of 0.1%, 0.2%, 0.4% and 0.9%. Therefore, a set of considerable amounts of data has been collected and the associated parameters have been analyzed. On the basis of the results already presented in previous sections, the main findings are as follows:

1. Experimental velocity isovel plots and transverse velocity distributions have been presented for uniform flow conditions.
2. The isovel plots (e.g. Figure 3) are generally symmetric, except in the central region where a local maximum occurs. However, it seems that the generally symmetrical distributions of primary flow are sometimes unstable, so that an alternative pattern of asymmetry may form. Such an alternating pattern is random for different flow conditions, being affected by secondary flow cells, which make the flow 3D. The random or stochastic nature of a fundamental instability in the flow field was also seen in the data of Powell & Posey [25,26] and Wasley [27]. In their experiments on the velocity distribution in a long prismatic triangular 90^o channel with uniform flow, Powell & Posey [25,26] found that, even after 20 to 120 Pitot tube manometer readings, taken at each of more than 60 locations, the resulting plots of averaged longitudinal velocity were not symmetrical.
3. The depth-wise velocity profiles tend towards the centerline of the channel near the water surface (see Figure 4). This finding is one of the strongest evidences for the presence of secondary currents. It is more apparent for the higher Froude numbers, Fr.
4. The logarithmic velocity law developed for a wide open channel has been shown to be largely ineffective for the current channel shape (see Figure 5).
5. The distributions of depth-averaged velocity show that they are fairly flat for low Froude numbers (see Figures 6a and 6b). This is not the case for higher Froude numbers.
6. There is a good linear relationship between the maximum velocity, u_{max}, and section mean velocity, U, which is given by Equations 6 and 7 (see Figure 7).
7. The depth-wise position of maximum velocity is shown to be near the surface for low Froude numbers. The filament of maximum velocity is depressed below the free surface as the Froude number increases.
8. The information in this paper may prove useful to any computational models dealing with channels having a similar channel shape. The work may also be valuable to river engineers trying to solve stable channel problems, as well as sediment transport in channels with side slopes, similar to channels with a V-shaped bottom.

ACKNOWLEDGMENTS

The author would like to express his thanks to Professor D.W. Knight from the University of Birmingham for his valuable comments and to the University of Urmia for funding the research expenses.

REFERENCES

1. Nezu, I. and Nakagawa, H., *Turbulence in Open-Channel Flows*, IAHR-Monograph, Balkema, Publishers, Rotterdam, Netherlands (1993).
2. Mohammadi, M. "Resistance to flow and the influence of boundary shear stress on sediment transport in smooth rigid boundary channels", PhD Thesis, School of Civil Engineering, The University of Birmingham, England (1998).
3. Balachandar, R., Hagel, K. and Blakely, D. "Velocity distribution in decelerating flow over rough surfaces", *Canadian Journal of Civil Engineering*, NRC Research Press, **29**(2), pp. 211-221 (April 2002).
4. Schlichting, H., *Boundary Layer Theory*, Seventh Ed., McGraw-Hill Classic Text Book Series, New York (1979).
5. Knight, D.W., Omran, M. and Tang, X. "Modeling depth-averaged velocity and boundary shear in trapezoidal channels with secondary flows", *J. Hydr. Engrg.*, **133**(1), pp. 39-47 (Jan. 2007).
6. Shiono, K. and Knight, D.W. "Turbulent open channel flows with variable depth across the channel", *J. Fluid Mechanics*, **222**(10), pp. 617-646 (1991).
7. Dermisis, D.C. and Papanicolaou, A.N. "Determining the 2-D surface velocity field around hydraulic structures with the use of a large scale particle image velocimetry (LSPIV) technique", *Proceedings World Water Congress*, **173**, p. 404 (2005).
8. Wilkerson, G.V. and McGahan, J.L. "Depth-averaged velocity distribution in straight trapezoidal channels", *J. Hydr. Engrg.*, **131**(6), pp. 509-512 (June 2005).
9. Chen, X. and Chiew, Y.-M. "Velocity distribution of turbulent open-channel flow with bed suction", *J. Hydr. Eng.*, **130**(2), pp. 140-148 (Feb. 2004)
10. Patra, K.C., Srijib, K.K. and Bhattacharya, A.K. "Flow and velocity distribution in meandering compound channels", *J. Hydr. Engrg.*, **130**(5), pp. 398-411 (May 2004).
11. Moramarco, T., Saltalippi, C. and Singh, V.P. "Estimation of mean velocity in natural channels based on Chiu's velocity distribution equation", *J. Hydrologic Engrg.*, **9**(4), pp. 42 (2004).
12. Mohammadi, M. "Velocity distribution in a V-shaped channel", *Proceeding the 2nd International Conference on Fluvial Hydraulics (Riverflow2004)*, Naples, 23-25 June, Italy. http://www.riverflow2004.unina.it/ (2004a)
13. Mohammadi, M. "Distribution of eddy viscosity in open channels", *Proceeding the 10th Asian Congress on Fluid Mechanics (ACFMX)*, Peradeniya University, 17-21 May, Kandy, Sri Lanka. http://acfmx.pdn.ac.lk/ (2004b).
14. Yang, S.-Q., Tan, S.-K. and Lim, S.-Y. "Velocity distribution and dip-phenomenon in smooth uniform open channel flows", *J. of Hydraulic Engineering, ASCE*, **130**(12), pp. 1179-1186 (2004).
15. Berlamont, J.E., Trouw, K. and Luyckx, G. "Shear stress distribution in partially filled pipes", *J. Hydr. Engrg.*, **129**(9), pp. 697 (2003).
16. Carollo, F.G., Ferro, V. and Termini, D. "Flow velocity measurements in vegetated channels", *J. Hydr. Engrg.*, **128**(7), pp. 664-673 (July 2002).
17. Proust, S., Rivière, N., Bousmar, D., Paquier, A. and Morel, R. "Velocity measurements in a concrete experimental channel representing a flood plain", *Hydraulic Measurements and Experimental Methods Conference 2002- HMEM*, Tony L. Wahl, Clifford A. Pugh, Kevin A. Oberg, Tracy B. Vermeyen, Eds., July 28-August 1, Estes Park, Colorado, USA (2002).
18. Babaeyan-Koopaei, K., Ervine, D.A., Carling, P.A. and Cao, Z. "Velocity and turbulence measurements for two overbank flow events in river severn", *J. Hydr. Engrg.*, **128**(10), pp. 891-900 (Oct. 2002).
19. Knight, D.W. and Sterling, M. "Boundary shear in circular pipes running partially full", *J. Hydr. Engrg.*, **126**(4), pp. 263-275 (April 2000).
20. Yannopoulos, P.C. and Demetracopoulos, A.C. "Contributions towards the prediction of velocity distribution in open channel flows", *Computer Methods in Water Resources XII*, **2**, Transaction: *Ecology and the Environment*, C.A. Brebbia, V.N. Burganos, G.P Karatzas and G. Pinder, Eds., **24**, p. 704 (1998).
21. González, J.A., Melching, C.S. and Oberg, K.A. "Analysis of open-channel velocity measurements collected with an acoustic doppler current profiler", *Proceedings 1st International Conference on New/Emerging Concepts for Rivers*, Organized by the International Water Resources Association, September 22-26, Chicago, Illinois, USA (1996).
22. Alhamid, A.A.I. "Boundary shear stress and velocity distributions in differentially roughened trapezoidal open channels", PhD Thesis, University of Birmingham, Birmingham, England (1991).
23. Mohammadi, M. and Knight, D.W. "Boundary shear stress distribution in a V-shaped channel", *Proceedings First International Conference on: Hydraulics of Dams & River Structures (HDRS)*, Esteghlal Hotel, Tehran, pp. 401-410, 26-28 April, Iran. http://hdrs.pwit.ac.ir/ (2004).
24. Mohammadi, M. and Knight, D.W. "Threshold condition for a V-shaped channel", *Proceeding XXVIII IAHR Congress*, Graz, Austria (1999).
25. Posey, C.J. and Powell, R.W. "Water surface profiles and velocity distributions for flow in a long uniform

channel", *Rocky Mountain Hydraulic Laboratory Report*, **26** (April 1961).

26. Powell, R.W. and Posey, C.J. "Resistance experiments in a triangular channel", *J. Hydraulic Div., ASCE*, **185**, (HY5) (May 1959).
27. Wasley, R.J. "Uniform flow in a shallow, triangular open channel", *J. Hydraulics Div., ASCE*, **87**(HY5) (Sept. 1961).
28. Tominaga, A., Nezu, I., Ezaki, K., and Nakagawa, H. "Three-dimensional turbulent structure in straight open channels", *J. of Hydr. Research*, **27**(1), pp. 149-173 (Aug. 1989).
29. Nezu, I. and Rodi, W. "Open channel flow measurement with a laser doppler anemometer", *J. of Hydr. Eng., ASCE*, **112**(5), pp. 335-355 (May 1986).
30. Streeter, V.L. and Wylie, E.B., *Fluid Mechanics*, McGraw-Hill Inc., NY (1979).
31. Chiu, C.-L. "Entropy and probability concepts in hydraulics", *J. Hydraulic Engineering, ASCE*, **113**(5), pp. 583-600 (1987).
32. Chiu, C.-L. "Entropy and 2-D velocity distribution in open channels", *J. Hydr. Eng., ASCE*, **114**(7) (July 1988).
33. Chiu, C.-L. "Velocity distribution in open channel flow", *J. Hydr. Eng., ASCE*, **115**(5) (May 1989).
34. Chiu, C.-L. and Murray, D.W. "Variation of velocity distribution in nonuniform open channel flow", *J. Hydr. Eng., ASCE*, **118**(7), pp. 989-1001 (July 1992).
35. Chiu, C.-L., Lin, G.-F. and Lu, J.-M. "Application of probability and entropy concept in pipe flow study", *J. Hydr. Eng., ASCE*, **119**(6), pp. 742-756 (June 1993).
36. Chiu, C.-L. and Abidin Said, C.A. "Modelling of maximum velocity in open-channel flow", *Proc. Hydraulic Div. Conf.*, **1**, pp. 381-385, New York (1994).
37. Chiu, C.-L. and Abidin Said, C.A. "Maximum and mean velocities and entropy in open-channel flow", *J. Hydraulic Eng., ASCE*, **121**(1), pp. 26-35 (Jan. 1995)
38. Xia, R. "Relation between mean and maximum velocities in a natural river", *J. Hydraulic Eng., ASCE*, **123**(8), pp. 720-723 (Aug. 1997).
39. Sterling, M. "The distribution of boundary shear stress in an open channel circular conduit running part-full", PhD Thesis, University of Birmingham, Birmingham, England (1997).